RSC Advances

ROYAL SOCIETY OF CHEMISTRY

www.rsc.org/advances

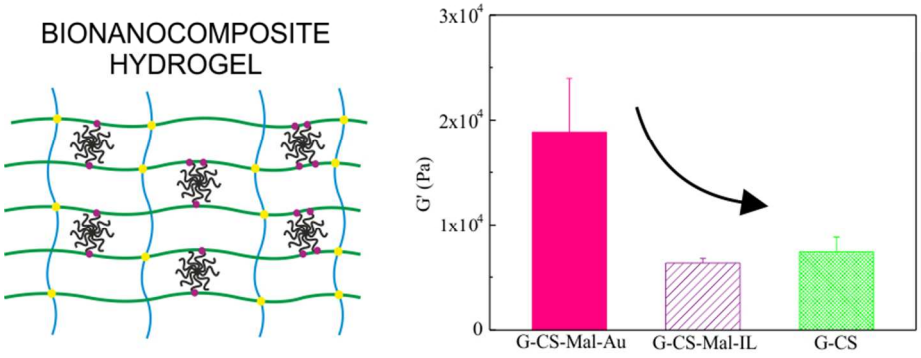

80x35mm (300 x 300 DPI)

RSC Advances

RSCPublishing

ARTICLE

EFFECT OF MALEIMIDE-FUNCTIONALIZED GOLD NANOPARTICLES ON HYBRID BIOHYDROGELS PROPERTIES

Cite this: DOI: 10.1039/xoxxoooooox

Received ooth January 2012,
Accepted ooth January 2012

DOI: 10.1039/xoxxoooooox

www.rsc.org/

C. García-Astrain,[a] I. Ahmed,[b] D. Kendziora,[b] O. Guaresti,[a] A. Eceiza,[a] L. Fruk,[b] M.A. Corcuera[a] and N. Gabilondo[a] ,

The role of well-dispersed gold nanoparticles as cross-linking agents in nanocomposite hydrogel formation was studied. Maleimide-coated gold nanoparticles were synthesized and used for Diels-Alder cycloaddition with furan modified gelatin. Hydrogel formation was aided by additional amide coupling of the modified gelatin with chondroitin sulfate. The cross-linking ability of the functionalized nanoparticles was evaluated and the final hydrogel properties were compared to those of a hybrid hydrogel containing inert-linker coated gold nanoparticles. The storage modulus of the nanoparticle cross-linked nanocomposites was 2.5-3 times compared to the controls. The presence of nanoparticles also affected the swelling properties, resulting in lower swelling ratios due to the formation of the more cross-linked structures. Conducted drug delivery experiments and the study of the light irradiation on the drug release behavior revealed promising features for the applications of nanocomposite polymer for drug delivery.

Introduction

The design of nanocomposite hydrogels (NC hydrogels) from natural polymers and inorganic nanoparticles for biotechnological and biomedical applications is attracting lots of interest from the wider scientific community.[1] In general, hydrogels are soft materials characterized by the absorption of huge amounts of water while maintaining their three-dimensional structure.[2] Comparing with conventional cross-linked hydrogels, NC hydrogels exhibit extraordinary mechanical, optical and swelling/deswelling properties.[3] Thanks to their unique characteristics and biocompatibility they have already been used for tissue engineering and drug delivery applications.[4,5]

Gold nanoparticles (Au NPs) have been employed in a number of biomedical applications such as drug delivery, sensor design or photothermal therapy, due to their stability, low toxicity[6] and electronic and optical properties.[7,8] Commonly, the incorporation of the NPs into the hydrogel is achieved either by their addition during the network formation by mixing[9] or through the "in situ" growth of the particles into the polymeric matrix.[10] Recently, Daniel-da-Silva et al. prepared thermoresponsive genipin-cross-linked gelatin hydrogels containing Au NPs after blending a gold colloid with gelatin and studied the effect of laser irradiation on the release of encapsulated methylene blue.[11] In another example, Heo et al. designed photo-curable gelatin hydrogels containing gold nanoparticles and showed remarkable ability to enhance the bone tissue repair.[12]

However, the mere physical incorporation within the hydrogel could lead to a continuous uncontrolled release of NPs to the surrounding environment, which could result in NPs accumulation with a potential toxic effect.[13] In order to avoid such release and design a new generation of enhanced NC hydrogels, it is desirable that the inorganic NPs act as multifunctional cross-linkers[3] covalently bound to the polymeric chains and taking active part in the establishment of a three-dimensional network.[14,15] Recently, Moreno et al. synthesized Au NPs (5-7 nm) functionalized with carboxylic groups for the cross-linking of poly (vinyl alcohol) through an esterification reaction.[16] Skardal et al. prepared cross-linked thiol-modified gelatin-hyaluronic acid hydrogels using 24 nm Au NPs as multivalent cross-linkers for applications in bioprinting.[17] The modification and use of NPs as hydrogel cross-linkers has been also applied to other types of nanoparticles such as $CoFe_2O_4$, Fe_3O_4 or TiO_2 and various hydrogel precursors.[15, 18-20] These strategies lead to chemically cross-linked hydrogel networks with good mechanical properties and structural integrity, in which the leaching of NPs is minimized during their subsequent use within various platforms.[21]

In our previous work we studied the applicability of the Diels-Alder (DA) "click" reaction for the design of hybrid hydrogels from gelatin and chondroitin sulfate (CS) using benzotriazole-maleimide-coated silver NPs.[22] Herewith we demonstrate the role of maleimide-functionalized Au NPs as multifunctional cross-linkers by comparing the final hydrogel properties with those of hybrid hydrogel containing only inert linker-coated Au NPs. Gelatin, a natural polymer derived from the partial hydrolysis of collagen, was chosen due to its biodegradable and biocompatible properties.[23] The same is true for CS, which is a predominant component of the extracellular matrix and mee

both structural and biological requirements for biomaterials synthesis. In order to bind the NPs to the polymer chains, gelatin was modified with furan groups through the free ε-amino groups (mainly in lysine and hydroxylysine residues) to allow for the Diels-Alder cycloaddition.[24] Additionally, second cross-linking, based on the amide coupling between CS and gelatin was employed to stabilize the hydrogel.[25]

Au NPs have previously been used for Diels-Alder reaction between furan and maleimide dodecanothiolate-modified monolayer-protected NPs for the preparation of reversible three-dimensional networks.[26] However, to the best of our knowledge, this is the first time that hybrid hydrogels were prepared by Diels-Alder reaction using Au NPs as cross-linkers for gelatin chains. To enable that, Au NPs were synthesized using a one-pot methodology employing bifunctional thiooctic acid-maleimide linkers anchored to the NPs surface.[27] In order to confirm the role of maleimide-coated NPs as cross-linkers, thiooctic acid-inert linker-coated NPs were also prepared for comparison. The nanocomposite hydrogel containing Au NPs showed remarkable viscoelastic properties and was explored for the design of a drug delivery platform.

Experimental Section

Materials

Gelatin (from porcine skin Type A, ≈ 300 Bloom), furfuryl glycidyl ether (FGE, 96.0%), chondroitin sulfate A sodium salt from bovine trachea (CS, ≥ 60.0%), gold (III) chloride hydrate ($HAuCl_4$, ≥ 99.9%), N-hydroxysuccinimide (NHS, 98.0%), N-(3-dimethylaminopropyl)-N'-ethylcarbodiimide hydrochloride (EDC, 99.0%) and sodium borohydride ($NaBH_4$, ≥ 99%) were purchased from Sigma-Aldrich. Phosphate buffered saline (PBS) solution was prepared from PBS tablets from Panreac (pH= 7.4). Deionized water was employed as solvent. All reagents and solvents were employed as received.

The modification of gelatin with furan units (G-FGE) was performed as described in our previous work.[24] Typically, gelatin was reacted with FGE in aqueous solution at basic pH at 55 ºC for 24 h. The solution was then neutralized and purified by dialysis against water. After freeze-drying, G-FGE was recovered as a yellowish solid.

Syntheses

Synthesis of maleimide linkers LA-TEG-Mal and LA-TEG-IL. Maleimide linkers N-(21-(2,5-dioxo-2,5-dihydro-1H-pyrrol-1-yl)-10-oxo-3,6,13,16,19-pentaoxa-9-azahenicosyl)-5-(1,2-dithiolan-3-yl)pentanamide (LA-TEG-Mal, 8) and inert linkers 2-(2-(2-methoxyethoxy)ethoxy)ethyl 5-(1,2-dithiolan-3-yl)pentanoate (LA-TEG-IL, 10) were prepared as depicted in Scheme 1. Details on the synthesis of each component are presented in ESI.

Synthesis of maleimide-coated gold nanoparticles (Mal-Au NPs). The synthesis of maleimide-coated gold nanoparticles (Scheme 2) was carried out following an already reported procedure with some modifications.[27,28] The following conditions were used to prepare Mal-Au NPs. 156 µL of a 50.8 mM solution of $HAuCl_4$ and 79.2 µL of 10 mM linker mixture solution (molar ratio of LA-TEG-Mal to LA-TEG-IL = 1:10) were dissolved in 25 mL of deionized water (final molar ratio of Au to linker mixture = 10:1). The mixture was stirred at room temperature for 1 h and 72 µL of 800 mM $NaBH_4$ stock solution in deionized water were added (in 18 µL aliquots) over a 30 min period under vigorous stirring. The mixture was then left stirring overnight resulting in a brown-red solution. Inert linker-coated gold nanoparticles (IL-Au NPs) were also prepared following the same procedure except from the fact that the linker solution contained only LA-TEG-IL.

Hydrogel formation. 180 mg of G-FGE were dissolved in 800 µL of Mal-Au NPs solution and CS was added in a 1:2 weight ratio with respect to G-FGE. 80.0 mg of EDC and 53.2 mg of NHS were added to the mixture which was allowed to gel for 1 h in a UV lamp at 254 nm (G-CS-Mal-Au). The Diels-Alder reaction between Mal-Au NPs and G-FGE and amide coupling between G-FGE and CS are depicted in Scheme 3. Two hydrogel controls were prepared using the same procedure, one using inert linker-coated gold nanoparticles (G-CS-IL-Au) and the other was made in absence of nanoparticles (G-CS). Thus, IL-Au NPs solution was used in the case of G-CS-IL-Au and deionized water in the case of G-CS.

Characterization

UV-vis Spectroscopy. The nanoparticle solution was analyzed by UV-vis Spectroscopy using a UV-3600/3100 from Shimadzu operating in a scan range of 200 to 600 nm with a 1 cm optical path quartz cuvette.

Scanning Electron Microscopy. Scanning Electron Microscopy (SEM) experiments were performed by a JEOL JSM-6400 with a wolframium filament operating at an accelerated voltage of 20 kV and at a working distance of 15 mm. Freeze-dried samples were coated with approximately 20 nm of chromium using a Quorum Q150 TES metallizer.

Transmission Electron Microscopy. Transmission Electron Microscopy (TEM) analysis of Au nanoparticles was performed using a transmission electron microscope TECNAI G2 20 TWIN (FEI), operating at an accelerating voltage of 200 KeV in a bright-field image mode. A solution drop was deposited on a carbon film copper grid and the sample was spin coated. In order to perform the TEM analysis of the nanocomposite hydrogel, samples were prepared by casting the hydrogel solution using the same procedure as described for nanoparticles solution. The hydrogel films were allowed to cure for 1 h under UV light (254 nm).

Rheology. Dynamic rheological behavior of the hydrogels was measured with a Rheometric Scientific Advanced Rheometric Expansion System (ARES), using parallel plate geometry (25 mm diameter). Frequency sweep measurements were performed at 37 ºC from 0.1 to 500 rad/s at a fixed strain in the linear viscoelastic region, previously assessed for each hydrogel by strain sweep experiments. Hydrogel samples were prepared in the form of disks of 25 mm diameter.

Swelling. Swelling capacity of freeze-dried hydrogels was studied by a general gravimetric method. Samples (n=3) were incubated in deionized water, physiological solution (NaCl 0.9% w/v), simulated gastric fluids (HCl 0.1M) and simulated intestinal fluid (phosphate buffer (PBS), pH= 7.4). At selected time intervals of 0.5, 1, 1.5, 2, 24 and 48 h, the swollen hydrogels were removed, the excess of liquid absorbed with a filter paper, and weighed. Hydrogels were then replenished with fresh solution. The swelling ratio (SR) was calculated using equation 1:

$$SR\,(\%) = \frac{(W_s - W_d)}{W_d} \cdot 100 \qquad (1)$$

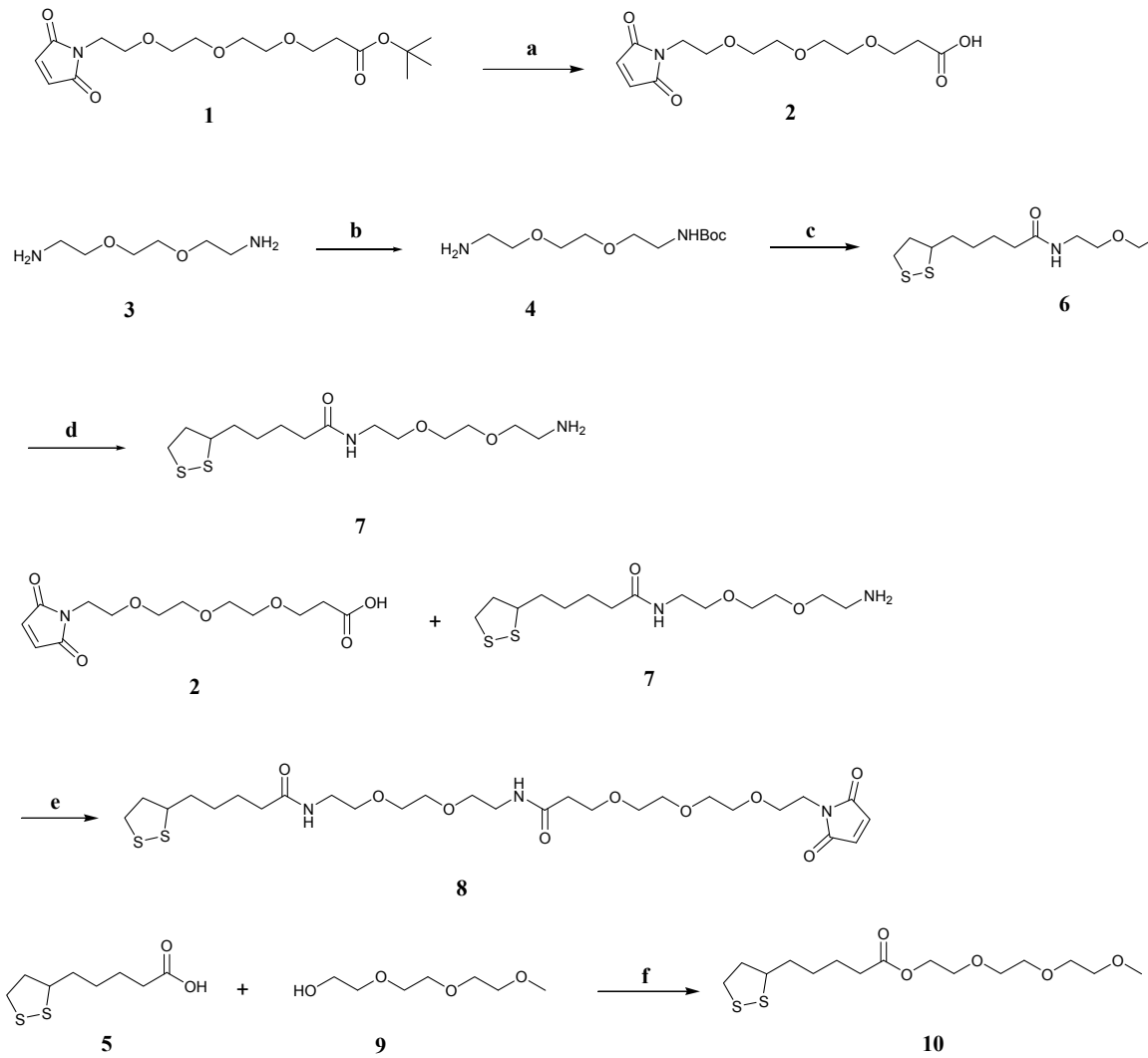

Scheme 1. Synthesis of LA-TEG-Mal (8) and LA-TEG-IL (10). Schematic representation of the organic synthesis a) TFA, CH_2Cl_2, RT, 2 h, b) di-tert-butyl dicarbonate, CH_2Cl_2, 0 ^{0}C, 6 h, RT, overnight, c) lipoic acid, TBTU, HOBt, DIPEA, THF, RT, overnight, d) TFA, CH_2Cl_2, RT, 2 h, e) TBTU, EDIPA, CH_2Cl_2, RT, 3 h, f) DCC, DMAP, CH_2Cl_2, RT, 12 h.

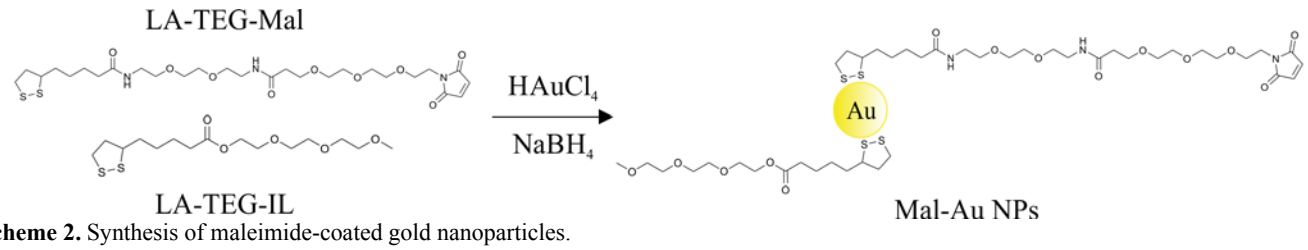

Scheme 2. Synthesis of maleimide-coated gold nanoparticles.

where W_s and W_d are the weight of the swollen and dried hydrogel samples respectively.

The equilibrium swelling was considered to be achieved when the weight of the hydrogels no longer increased.

Drug delivery experiments. Antibiotic chloramphenicol (ClPh) was used as a model drug namely because its water-solubility and its wide antibacterial spectrum.[28] Freeze-dried samples of the hydrogels were loaded by soaking a 0.25 mg/mL aqueo solution of ClPh at 25 ºC. Based on the equilibrium swelling times from the swelling studies, hydrogels were maintained in the drug solution for 3 h. After that time, the gel sample w removed from the solution, dried at ambient temperature and weighed.

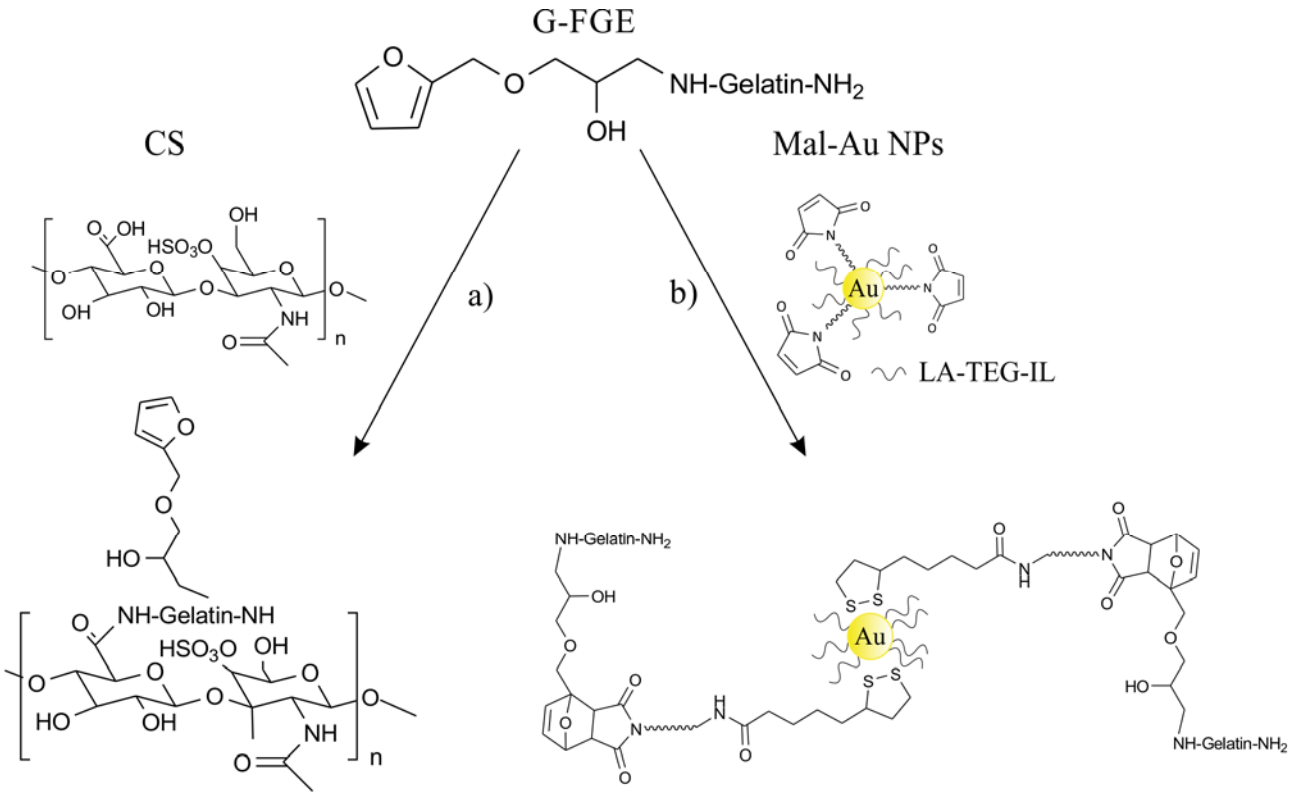

Scheme 3. Hydrogel formation reactions; path a) amide coupling between CS and Gel-FGE in the presence of EDC and NHS and path b) DA reaction between G-FGE and maleimide-coated Au NPs.

The amount of drug loaded was determined from the amount of drug solution absorbed by the hydrogel, calculating the difference between the initial dried weight of the sample and the final weight after loading. The release experiments were carried out by shaking the dried loaded hydrogel samples (kept in a metallic perforated bag) in 80 mL of PBS 0.01 M pH = 7.4 at 37 ºC. After predetermined time intervals, 1.0 mL of the release medium was withdrawn and analyzed by UV-vis spectroscopy to determine the amount of drug released at each time point, returning the aliquot to the beaker once analyzed. The amount of ClPh released was quantified by comparing the absorbance at 275 nm (maximum absorbance of ClPh) with a standard calibration curve prepared for pure drug solutions in the appropriate concentration regions. The cumulative drug release was calculated using equation 2:

$$\text{Cumulative Release}\,(\%) = \frac{m_t}{m_0} \cdot 100 \qquad (2)$$

where m_t is the cumulative mass of ClPh released at time t and m_0 is the total amount of ClPh loaded.

Drug release experiments were also performed under UV irradiation at 254 nm. Hydrogel samples were loaded following the same procedure as mentioned above. In a typical experiment, dried hydrogel samples were immersed in 80 mL of PBS solution 0.01 M pH = 7.4 at ambient temperature and kept in a UV lamp (254 nm). Aliquots were taken after 1 and 2 h of light irradiation and the absorbance was measured in a UV-vis spectrophotometer as described previously. For comparison, control experiments were also performed in the same conditions in the absence of light irradiation.

Results and Discussion

Synthesis and characterization of Mal-Au NPs

The functionalization of the Au NPs with appropriate groups is necessary for the synthesis of hybrid hydrogels incorporating NPs as cross-linking agents. To enable Diels-Alder cycloaddition with furfuryl-gelatin, maleimide-functionalized Au NPs were prepared using a one-pot procedure employing $HAuCl_4$ precursor, $NaBH_4$ as reducing agent and thiooctic acid-based linkers.[28,30] For Mal-Au NPs synthesis, a mixture of LA-TEG-Mal (8) and LA-TEG-IL (10) linkers was used, whereas only LA-TEG-IL (10) linker was employed to obtain control IL-Au NPs.[27,28] Formation of Au NPs was confirmed by UV-vis spectroscopy, due to the appearance of plasmon resonance peak characteristic for Au NPs around 520 nm (Fig. 1A).[31] Both the average diameter (appr. 5 nm) and the concentration of the functionalized Mal-Au NPs (0.18 µmol/L) and IL-Au NPs (0.16 µmol/L) were determined from UV-vis spectra using previously described procedures and literature extinction coefficient.[31]

NPs were additionally characterized by TEM (Fig. 1B and C) and the average diameters of spherical NPs were estimated to 4.7 ± 1.1 and 4.9 ± 1.4 nm for Mal-Au NPs and IL-Au NPs, respectively. There were also no aggregates observed, confirming their colloidal stability.

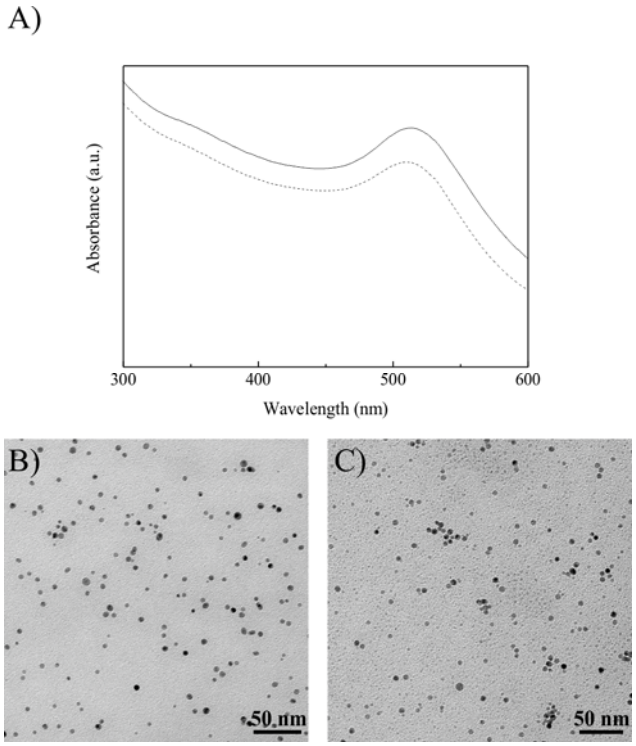

Figure 1. A) UV-vis spectra of Mal-Au NPs (straight line) and IL-Au NPs (dashed line), B) TEM image of Mal-Au NPs and C) TEM image of IL-Au NPs.

Hydrogel synthesis and characterization

The synthesis of the hydrogels involved two different cross-linking reactions to guarantee hydrogel formation. On one hand, Diels-Alder reaction between the furan groups of furfuryl gelatin G-FGE and the maleimide groups of Mal-Au NPs in aqueous solution was employed. Although number of experiments were performed using only Mal-Au NPs, hydrogels of unsatisfactory stability were obtained. Therefore, additional cross-linking reaction amide coupling between free primary ε-amino groups of gelatin, i. e. those that were not substituted with FGE and carboxylic groups of CS in the presence of EDC and NHS was allowed to take place. After both chemical reactions were performed, the cross-linked stable NC hydrogel containing covalently bonded gold nanoparticles was obtained. In Fig. 2, three different types of prepared hydrogels are shown; G-CS-Mal-Au with cross-linked Au NPs and control hydrogels, G-CS-IL-Au containing inert linker-coated Au NPs and G-CS without NPs.

It can be observed that, for G-CS-IL-Au and G-CS hydrogels, the consistency of the material is different from that of G-CS-Mal-Au, resulting in viscous and sticky hydrogels. However, when Au NPs were used as cross-linkers, solid-like and elastic samples were obtained and the sample retained the disc-shape of the container used for its preparation.

The presence and distribution of NPs within G-CS-Mal-Au hydrogel was confirmed by TEM (Fig. 3) and it can be seen that NP are dispersed into the hydrogel matrix and there is no observable particle aggregation.

The microstructure of both the nanocomposite hydrogel and the control was studied by means of SEM. Both SEM images of freeze dried (Fig.4a and c) and PBS swollen samples prior to freeze drying (Fig. b and c) were obtained. As it can be observed, the morphology after swelling of both Au containing and control samples is altered. It has to be taken into account that non-swollen hydrogels contain only water, which is present during the synthesis and after the swelling process in PBS solution their liquid content is significantly higher and this affects the microstructure of the network. For both the control (Fig. 4a) and Au containing hydrogel (Fig. 4c) after freeze drying, similar homogeneous compact structures containing smooth areas and regions with pits and grooves can be observed. However, upon swelling, the morphology of G-CS (Fig. 4b) and G-CS-Mal-Au (Fig. 4d) is considerably different.

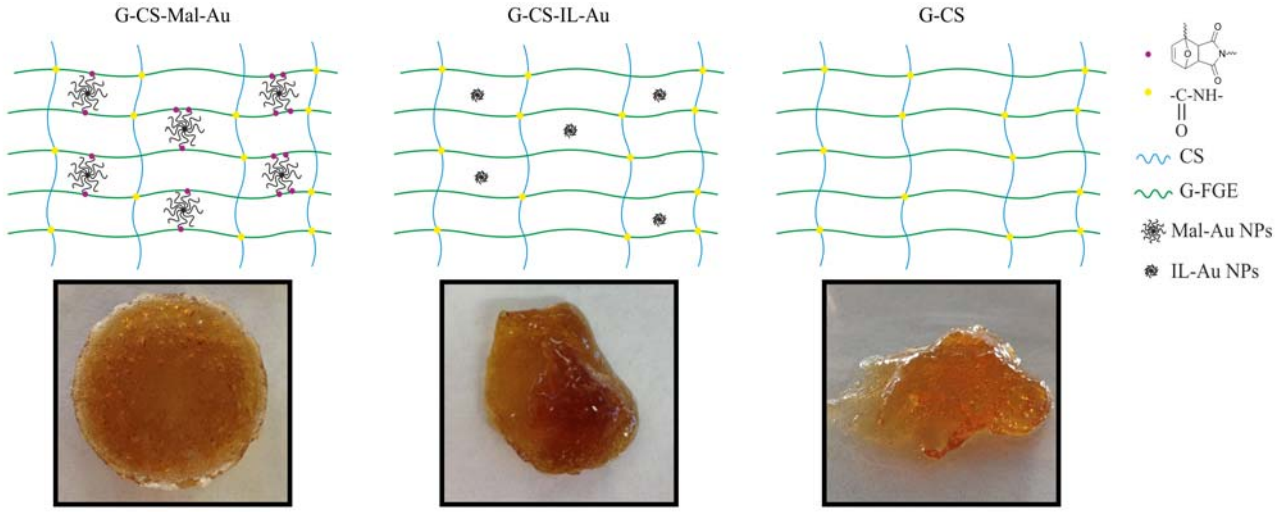

Figure 2. Scheme of the network structure and hydrogel pictures

In G-CS hydrogel smooth areas as well as bumps and striated regions were observed whereas the surface of G-CS-Mal-Au hydrogel is more homogeneous and highly wrinkled with random pores.

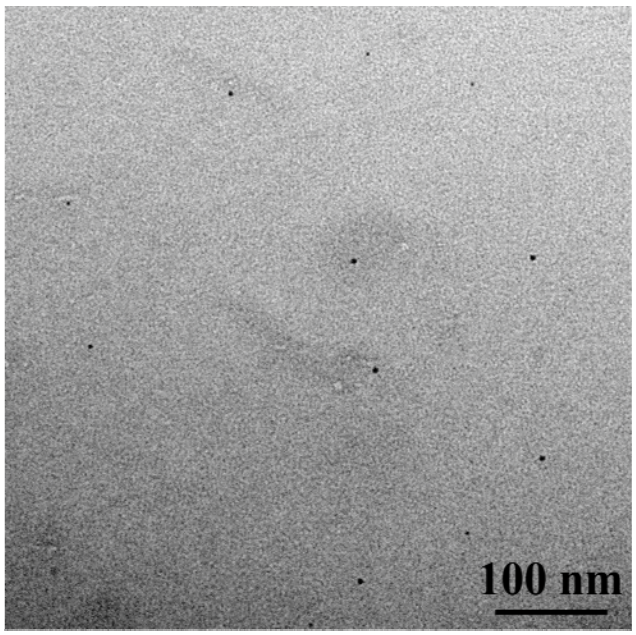

Figure 3. TEM image of the nanocomposite hydrogel G-CS-Mal-Au.

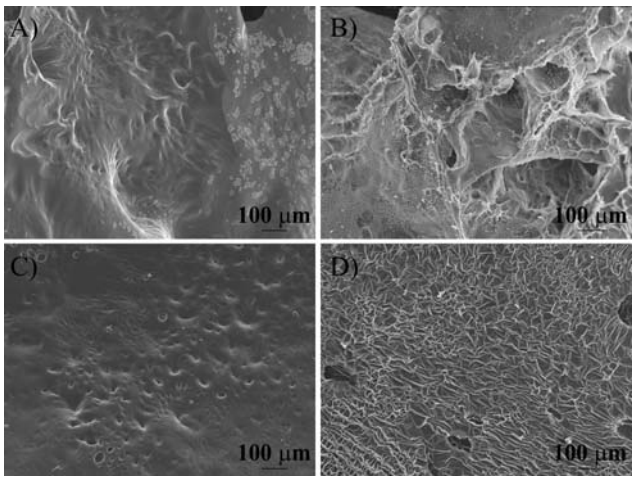

Figure 4. SEM images of freeze-dried hydrogels a) G-CS, b) G-CS swollen in PBS, c) G-CS-Mal-Au and d) G-CS-Mal-Au swollen in PBS.

Rheological measurements

The elastic properties of G-CS-Mal-Au hydrogel were characterized by dynamic rheological studies at 37 ºC using parallel plate geometry. All samples were previously submitted to strain sweep tests in order to establish the linear viscoelastic region where both the storage (G') and the loss modulus (G'') were independent of the applied strain. Fig. 5 shows that during the frequency sweep, G'' was considerably smaller than G', indicating the elastic nature of the network.

Moreover, hydrogels presented a characteristic rubbery pattern during the test, as G' was maintained constant within the frequency range used, denoting that they were chemically cross-linked prior to measurement[32] and confirming the efficacy of the cross-linking strategy. The mean G' values for the different hydrogel compositions studied are reported in Table 1. When comparing with the control without nanoparticles (G-CS), G-CS-Mal-Au hydrogel showed a dramatically higher G' value indicating, as it could be predicted, that the presence of the Au NPs into the hydrogel network played an important role in its rigidity. However, in order to verify that not only the metallic NPs acted as reinforcement at the nanoscale but also that their maleimide functionalization at the surface played a role, controls with inert linker-coated gold nanoparticles (IL-Au NPs) were also investigated (G-CS-IL-Au). As it can be observed, in the case of inert Au NP control, the G' value of G-CS-IL-Au hydrogel was close to that of the G-CS and considerably lower than that of G-CS-Mal-Au. As the employed NP suspensions were almost identical, we assume that the final NP concentration within both NC hydrogels is similar. This indicates that use of maleimide coated Au NPs, which engage in Diels-Alder reaction with furfuryl-gelatin results in a significantly stiffer network. The low G' values for G-CS-IL-Au hydrogel, very similar to that of the NP-free hydrogel, could be related to the very low effect of small inert Au NPs on the hydrogel matrix. It should also be noted that the concentration of the used NP was low compared to other published procedures,[14,15,18,19] which confirms that even a low amount of Au NP capable of cross-linking reactions has a significant effect on the resulting hydrogels and G' values. These nanoparticle cross-linked biopolymeric NC hydrogels arise as promising materials for biomedical applications since the mean values of the storage modulus were close from those of liver, fat, relaxed muscle and breast gland tissue (103-104 Pa).[33]

Swelling behavior

The role of gold nanoparticles as cross-linkers in the nanocomposite hydrogel was further confirmed through swelling experiments performed at 37 ºC in different media, water, HCl 0.1 M solution (simulating gastric fluids), NaCl 0.9% w/v (physiological solution) and PBS, pH = 7.4 (simulated intestinal fluid). Figure 6 shows the equilibrium swelling ratios as a function of the swelling media for the different hydrogel samples G-CS-Mal-Au and controls, G-CS-IL-Au and G-CS. G-CS and G-CS-IL-Au obtained in absence of NPs and with inert linker-coated NPs, respectively, showed the highest swelling ratio in all the media. It can also be noticed that the swelling ratio of G-CS-IL-Au hydrogel in water was significantly higher than the hydrogel alone. This could be explained by the hydrophilicity of the inert linker present in the surface of the Au NPs. In this hydrogel, the nanoparticles are not acting as cross-linkers, the network structure is similar to that of G-CS but more hydrophilic since TEG moieties are present, which contribute to the increase of the swelling ratio. On the other hand, in the case of G-CS-Mal-Au the swelling ratio was considerably reduced. The reason for this probably lies in Diels-Alder reaction as it has already been reported that highly cross-linked networks show lower swelling ratios.[34]
For all the hydrogels, the highest swelling ratios were obtained in water or in PBS solution. When immersed in physiological solution, swelling is reduced as the presence of salts could cause a screening effect, lowering the repulsion between G-FGE and CS chains and thus, the swelling. Finally, significantly

A)

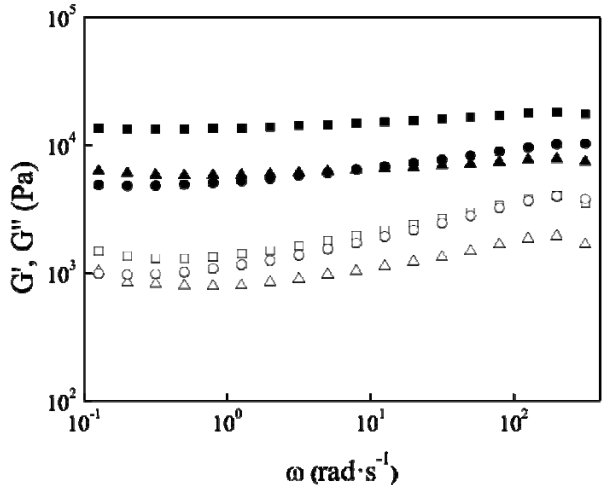

B)

SAMPLE	G' (Pa)	G'' (Pa)
G-CS-Mal-Au	18864.3 - 5110.0	2509.5 - 345.3
G-CS-IL-Au	6334.1 - 419.7	1246.8 - 110.5
G-CS	7381.8 - 1421.2	1564.0 - 567.4

Figure 5. A) Frequency Sweep of hydrogels (G' (filled symbols) and G'' (empty symbols). ■ G-CS-Mal-Au, ▲ G-CS-IL-Au, ● G-CS) and B) mean G' and G'' values at 37 ºC (Average ± Standard deviation, n = 3).

lower swelling ratios were observed for low pH. This behavior could be attributed to the increment of the number of associated carboxylic groups which are able to form inter and intra-molecular hydrogen bonding between gelatin chains and, subsequently, cause a decrease in the swelling ratio.[35]

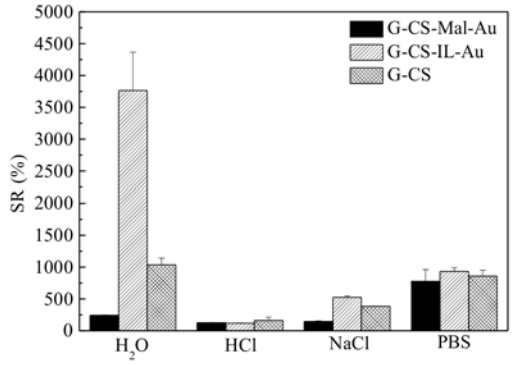

Figure 6. Equilibrium swelling data for G-CS-Mal-Au, G-CS-IL-Au and G-CS hydrogels while incubated in water, HCl (0.1 M), NaCl (0.9 %wt.) and PBS (pH = 7.4) solutions at 37 ºC.

Drug release

Finally, we were interested in exploring the remarkable properties of Au NP containing hydrogels for drug delivery. To achieve that, the release of the model drug, antibiotic chloramphenicol from G-CS-Mal-Au, G-CS-IL-Au and G-CS in PBS at 37 ºC was studied. The amount of ClPh released was monitored by ultraviolet spectroscopy and the cumulative release of ClPh was calculated using equation 2. The different hydrogel compositions showed very similar drug delivery profiles (Fig. 7). In all cases, there was an initial fast drug release achieving the steady concentration in the first hour, probably indicating that the drug is predominantly surface-associated for all the drug-loaded hydrogels. The release rate increased as follows G-CS<G-CS-IL-Au<G-CS-Mal-Au. It is worth noting that the three systems absorbed different amounts of ClPh solution due to their different swelling capacity. The calculated amounts of absorbed drug were 1.61 ± 0.07, 4.78 ± 0.47 and 9.28 ± 0.09 mg ClPh/g hydrogel for G-CS-Mal-Au, G-CS-IL-Au and G-CS, respectively. G-CS-IL-Au swelled more than G-CS in water but the amount of drug absorbed was smaller. This behavior could be related to the swelling rate, since G-CS reached the equilibrium swelling faster than G-CS-IL-Au. Moreover, the fact that hydrogel samples were swollen in drug solution at 25 ºC could explain the difference between the swelling ratio observed at 37 ºC and the amount of aqueous solution absorbed during drug loading.

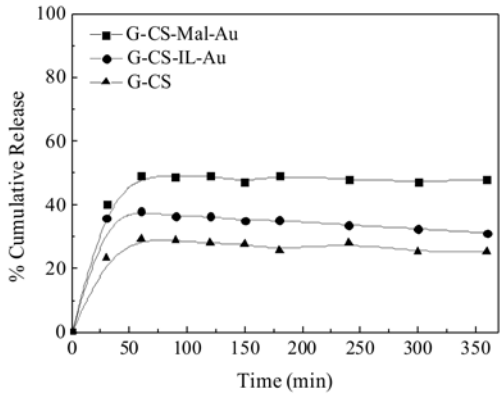

Figure 7. Release pattern of ClPh from ClPh-loaded G-CS-Mal-Au (■), G-CS-Il-Au (●) and G-CS (▲) hydrogels in PBS buffer at 37 ºC.

Regarding the cumulative drug release, it is worth noting that none of the hydrogel compositions released more than 50% of the loaded drug. G-CS-Mal-Au hydrogel released nearly 50% of the loaded drug, whereas G-CS-IL-Au and G-CS hydrogels released only 31 and 27% of drug, respectively. A strong electrostatic interaction could probably be the reason of the

scarce value of the total release percent in all samples. At the physiological pH, the results suggest that there is a strong electrostatic interaction between ClPh and the functional groups of gelatin and CS, which could hinder the drug release. This behaviour was also reported previously for gelatin-based hydrogels using chlorhexidine digluconate as the model drug[36]. As in the case of ClPh, the electrostatic interactions between the groups present in the polymeric framework and the drug are highly probable and, thus, the cumulative release reaches a plateau. This cumulative release would not be altered as long as the hydrolytic degradation of the matrix does no take place.

The difference in the structure of G-CS-Mal-Au compared to the G-CS could have an influence on the release capacity of the hydrogel, since more cross-linking points are present. G-CS-Mal-Au displayed lower swelling ratios and, thus, the diffusion of the drug into the matrix could be hindered. The drug would be predominantly trapped close to the surface areas favoring the release from the system. In the case of G-CS hydrogel the drug could better penetrate inside the matrix due to its high swelling ratio, making the release more difficult. The presence of Au-IL NPs also seemed to play a role in the release of ClPh since G-CS-IL-Au absorbed an intermediate amount of drug and the release efficiency was also between those of G-CS and G-CS-Mal-Au. Interactions between the inert linker present in the nanoparticle surface and the polymer matrix could alter the network structure and influence the release behavior.

We were also interested in studying if the drug release could be controlled by external stimuli such as light irradiations. It has been shown previously that irradiation can affect Au containing hydrogels due to the high hyperthermic effect shown upon interaction of Au NP plasmon with light.[37,38] Daniel-da-Silva et al. reported an increment of drug release after laser irradiation at 532 nm which matched the Surface Plasmon Resonance band of gold nanoparticles.[11] As it has been reported, after irradiation of the NPs, the produced local heating could induce transformations in the hydrogel structure, promoting the drug release.[11]

Fig. 8 shows the efficiency of ClPh release of the hydrogels after the exposure to UV irradiation of 254 nm, where it is known that the AuNPs also absorb.[39] The release was monitored for 1 and 2 h at room temperature and it can clearly be seen that the drug release from hybrid Au NP containing hydrogel was improved after light irradiation.

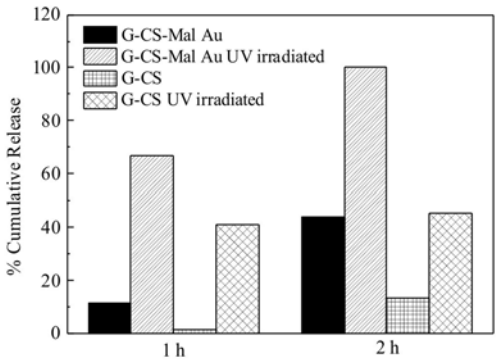

Figure 8. Drug release efficiency of G-CS-Mal Au and G-CS with and without UV irradiation.

When comparing to non-irradiated G-CS-Mal-Au control samples, the experimental results for G-CS-Mal-Au showed a 55% increase of the release efficiency after both 1 and 2 h of light irradiation. However, the effect of UV irradiation was also noticed for hydrogel controls without NPs, leading to higher amounts of drug released. A possible explanation of this finding could be the fact that UV irradiation was accompanied by a warming of the hydrogel, resulting in increased mobility of the polymeric chains, and, hence, the drug release is facilitated in comparison with non-irradiated samples. Future experiments will employ laser irradiation in the visible region to optimize the light induced release. Nevertheless, when comparing the drug release efficiency for G-CS and G-CS-Mal-Au hydrogels after irradiation, it can be observed that there was a further improvement of the release efficiency for Au NP-nanocomposite hydrogel. After irradiation, there is still a 15% and 25% increment in the release efficiency of G-CS-Mal-Au after 1 and 2 h of irradiation, respectively, in respect to the control G-CS. There is an important effect of UV light over the release rate which is more obvious for the first irradiation hour. This effect is also noticeable for the nanocomposite hydrogel during the second hour of irradiation whereas for G-CS hydrogel the release remains almost constant.

Conclusions

The effect of maleimide-coated gold nanoparticles on the cross-linking of furan-modified gelatin was investigated. Functionalized gold nanoparticles were prepared using derivatives containing thiootic moieties for Au binding and maleimide group for active cross-linking through Diels-Alder reaction. Stable hydrogels were formed after the Diels-Alder reaction of Au-Mal nanoparticles with furan containing gelatin and amide coupling of free gelatin amine groups with chondroitin sulfate. Obtained Au NP containing hydrogels were characterized with remarkable increase in the storage moduli values even though minute amounts of Au NPs were used in comparison with other published procedures. Additionally, the swelling studies further confirmed the role of maleimide-coated nanoparticles as multiple cross-linkers for the gelatin chains since the swelling properties were significantly altered. Finally, the release of the embedded model drug was studied and showed huge potential of the hybrid gels to act as drug delivery devices. Furthermore, even if future work regarding the biocompatibility of these materials needs to be addressed, remarkable properties of these novel hydrogels might be of huge significance for the development of other biomedical platforms such as tissue growth scaffolds or replacements materials.

Acknowledgements

Financial support from the Basque Country Government in the frame of Saiotek S-PE12UN036 and Grupos Consolidados (IT-776-13) and from the University of the Basque Country (UPV/EHU) in the frame of EHUA12/19 is gratefully acknowledged. C. G-As wishes to acknowledge the Universidad del País Vasco/Euskal Herriko Unibertsitatea (Ayudas para la Formación de Personal Investigador) for PhD grant PIFUPV10/034. L. F. acknowledges support of CFN Project A5.7. Moreover, technical and human support provided by SGIker (UPV/EHU, MINECO, GV/EJ, ERDF and ESF) is also gratefully acknowledged.

Notes and references

[a] 'Materials + Technologies' Group, Dept. of Chemical and Environmental Engineering, Polytechnic School, University of the Basque Country. Pza. Europa 1. 20018 Donostia-San Sebastián, Spain.
[b] DFG-Centre for Functional Nanostrucutres (CFN), Karlsruhe Institute of Technology, Wolfgang-Gaede Str. 1a, 76131 Karlsruhe, Germany.

1 C. Aimé and T. Coradin, *Journal of Polymer Science Part B: Polymer Physics*, 2012, **50**, 669.
2 J. Kopecek and J. Yang, *Polymer International*, 2007, **56**, 1078.
3 K. Haraguchi, *Current Opinion in Solid State and Materials Science*, 2007, **11**, 47.
4 X. Liu, L. A. Smith, J. Hu and P. X. Ma, *Biomaterials*, 2009, **30**, 2252.
5 C. A. Dermachi, A. Debrassi, F. de Campos Buzzi, R. Corrêa, V. C. Filho, C. A. Rodrigues, N. Nedelko, P. Demchenko, A. Slawska-Waniewska, P. Dłuzewski and J. M. Greneche, *Soft Matter*, 2014, **10**, 3441
6 J. Zhu, C. Waengler, R. B. Lennox and R. Schirrmacher, *Langmuir*, 2012, **28**, 5508.
7 G. L. Hallett-Tapley, M. J. Silvero, C. J. Bueno-Alejo, M. González-Béjar, C. D. McTiernan, M. Grenier, J. C. Netto-Ferreira and J. C. Scaiano, *The Journal of Physical Chemistry C*, 2013, **117**, 12279.
8 U. Saxena and P. Goswami, *Journal of Nanoparticle Research*, 2012, **14**, 813.
9 X. F. Sun, B. Liu, Z. Jing and H. Wang, *Carbohydrate Polymers*, 2015, **118**, 16.
10 K. M. Rao, K. S. V. K. Rao, G. Ramanjaneyulu, K. C. Rao, M. C. S. Subha and C. S. Ha, *Journal of Biomedical Materials Research A*, 2014, **102**, 3196.
11 A. L. Daniel-da-Silva, A. M. Salgueiro and T. Trindade, *Carbohydrate Polymers*, 2015, **118**, 16.
12 D. Nyoung Heo, W.K. Ko, M. Soo Bae, J. Bok Lee, D. W. Lee, W. Byun, C. Hoon Lee, E.C. Kim, B. Y. Jung and I. Keun Kwon, *Journal of Materials Chemistry B*, 2014, **2**, 1584.
13 M. Mahmoudi, A. Simchi and O.U. Hafeli, *Journal of Physical Chemistry C*, 2009, **113**, 8124.
14 R. Barbucci, D. Pasqui, G. Giani, M. De Cagna, M. Fini, R. Giardino and A. Atrei, *Soft Matter*, 2011, **7**, 5558.
15 R. Barbucci, G. Giani, S. Fedi, S. Bottari and M. Casolaro, *Acta Biomaterialia*, 2012, **8**, 4244.
16 M. Moreno, R. Hernández and D. López, *European Polymer Journal*, 2010, **46**, 2099.
17 A. Skardal , J. Zhang , L. McCoard , S. Oottamasathien and Glenn D. Prestwich, *Advanced Materials*, 2010, **22**, 4736.
18 D. Pasqui, A. Atrei, G. Giani, M. De Cagna and R. Barbucci, *Materials letters*, 2011, **65**, 392.
19 G. Giani, S. Fedi and R. Barbucci, *Polymers*, 2012, **4**, 1157.
20 R. Messing, N. Frickel, L. Belkoura, R. Strey, H. Rahn, S. Odenbach and A. M. Schmidt, *Macromolecules*, 2011, **44**, 2990.
21 Y. Zhou, N. Sharma, P. Deshmukh, R. K. Lakhman, M. Jain and R. M. Kasi, *Journal of the American Chemical Society*, 2011, **134**, 1630.
22 C. García-Astrain, C. Chen, M. Burón, T. Palomares, A. Eceiza, L. Fruk, M. A. Corcuera and N. Gabilondo, *Biomacromolecules*, 2015, **16**, 1301-1310.
23 K. M. Park, Y. Lee, J. Y. Son, D. H. Oh, J. S. Lee and K. D. Park, *Biomacromolecules*, 2012, **13**, 604.
24 C. García-Astrain, A. Gandini, C. Peña, I. Algar, A. Eceiza, M Corcuera and N. Gabilondo, *RSC Advances*, 2014, **4**, 35578.
25 A. J. Kuijpers, G. H. M. Engbers, T. K. L. Meyvis, S. S. C. de Smedt, J. Demeester, J. Krijgsveld, S. A. J. Zaat, J. Dankert and J. Feijen, *Macromolecules*, 2000, **33**, 3705.
26 J. Zhu, A. J. Kell and M. S. Workentin, *Organic Letters*, 2006, **8**, 4993.
27 D. M. Kendziora, I. Ahmed and L. Fruk, *RSC Advances*, 2014, **4**, 17980.
28 E. Oh, K. Susumu, R. Goswami and H. Mattoussi, *Langmuir*, 2010, **26**, 7604.
29 G. Buhus, C. Peptu, M. Popa and J. Desbrières, *Cellulose Chemistry and Technology*, 2009, **43**, 141.
30 E. Oh, K. Susumu, J. B. Blanco-Canosa, I. L. Medintz, P. E. Dawson and H. Mattoussi, *Small*, 2010, **6**, 1273.
31 W. Haiss, N. T. K. Thanh, J. Aveyard and D. G. Fernig, *Analytical Chemistry*, 2007, **79**, 4215.
32 C. García Astrain, A. Gandini, D. Coelho, I. Mondragon, A. Retegi, A. Eceiza, M.A. Corcuera and N. Gabilondo, *European Polymer Journal*, 2013, **49**, 3998.
33 J. L. Vanderhooft, M. Alcoutlabi, J. J. Magda and G. D. Prestwich, *Macromolecular Bioscience*, 2011, **12**, 824.
34 C. M. Nimmo, S. C. Owen, M. S. Shoichet, *Biomacromolecules*. 2009, **9**, 20-28.
35 A. I. Raafat, *Journal of Applied Polymer Science*, 2010, **118**, 2642.
36 N. J. Einerson, K. R. Stevens, W. J. Kao, Biomaterials, 2002, **24**, 509.
37 Y. Oni, K. Hao, S. Dozie-Nwachukwu, J. D. Obayemi, O. S. Odusanya, N. Anuku and W. O. Soboyejo, *Journal of Applied Physics*, 2014, **115**, 084305.
38 N. Niu, F. He, P. Ma, S. Gai, G. Yang, F. Qu, Y. Wang, J. Xu and P. Yang, *ACS Applied Materials and Interfaces,* 2014, **6**, 3250.
39 S. Sarina, E. R. Waclawik and H. Zhu, *Green Chemistry*, 2013, **15**, 1814.